Proceedings of the ASME 2010 3rd Joint US-European Fluids Engineering Summer Meeting and 8th International Conference on Nanochannels, Microchannels, and Minichannels
FEDSM-ICNMM2010
August 1-5, 2010, Montreal, Canada

FEDSM-ICNMM2010-31006

TRANSIENT RESPONSE OF SUBMERGED ELASTIC STRUCTURES SUBJECT TO UNDERWATER SHOCK WAVES

Zhanke Liu

15270 Voss RD
Sugar Land, TX 77498
Email: zhankeliu2008@gmail.com

Yin L. Young

Department of Naval Architecture and Marine Engineering
University of Michigan, Ann Arbor, MI 48109
Email: ylyoung@umich.edu

Abstract

This paper presents the transient response of submerged elastic structures subject to underwater shock waves. Two fundamental effects are investigated, namely, the inertial and elastic effects, characterized by two non-dimensional parameters, namely, the inertial parameter M and the elastic parameter K. Case studies are provided with physical and mathematical interpretations of the results.

1 Introduction

In the pioneering work of Taylor (1941), Taylor studied the fluid-structure interactions (FSI) between an exponentially decaying plane shock wave and an infinite rigid flat plate. Taylor's model of a floating air-backed plate remains the foundation for the understanding of FSI between underwater shock and floating structures. An enhancement of Taylor's treatment was presented in Hutchinson & Xue (2005) to account for the yield strength of the core to improve the estimation of momentum transmission to sandwich constructions. Extension of Taylor's model for air blast loading was accomplished in Kambouchev *et al.* (2006), where nonlinear compressibility effects are important.

Much of the previous work was focusing on air-backed structures. Recently, there was an increased interest in water-backed structures, driven by analysis and design of advanced composite marine propellers (Young, 2007, 2008; Liu, 2008; Liu & Young, 2009). In Liu & Young (2008), the influence of backing conditions (i.e. air-backed versus water-backed) was systematically analyzed. The solution of the water-backed plate (WBP) was cast into the same format as that of the air-backed plate (ABP) with a modified fluid-structure interaction (FSI) parameter to facilitate a unified analysis of the ABP and WBP using the same set of formulae. The influence of back conditions on fluid and structural dynamics, including fluid cavitation, was systematically investigated. Asymptotic limits were mathematically identified and physically interpolated. Results showed that the WBP experiences lower net pressure loading, reduced structural response, and hence lower peak momentum gaining. The time to reach peak momentum was shown to be shorter for the WBP than for the ABP. Cavitation was found to be almost inevitable for the ABP, while relevant to the WBP only for a small range of the FSI parameter.

Another important feature of underwater shock waves is their finite pressure rise time. Most of the previous studies, however, assumed 'steep front', namely, zero pressure rise time. More recently, Liu & Young (2010) performed detailed mathematical and physical analysis of submerged elastic plates (both air- and water-backed) subject to underwater shock loading with pressure precursor. Case studies showed that the pressure precursor significantly decreases the impact-side peak pressure of both air-backed and water-backed plates. At the same time, it leads to much earlier cavitation and peak momentum arrival.

Another phenomenon that was in general missing in previous studies is the influence of elastic support in terms of shock-structure interaction dynamics. The elastic effect was included

in the original work of Taylor (1941) for air-backed structures. However, elastic effect was not the primary focus of Taylor (1941). Instead, more discussions were based on the solution for freely standing structures. The current work is to derive the complete mathematical formulations for the transient responses of both *ABP* and *WBP* with elastic support subject to underwater shocks. Two fundamental effects, namely inertial and elastic effects, are identified and studied in the parametric space. The general solution is shown to be bounded by extreme cases with interesting intermediate response spectrums. Detail results are presented in the following sections.

2 Formulation

Consider a rigid plate of mass per unit area $m = \rho_s h_s$ with elastic support, where ρ_s and h_s are respectively the density and thickness of the solid plate. The elastic support is assumed to have an equivalent stiffness of k. Notice that the unit of k is $force/length^3$, namely stiffness per unit area. Thus the elastically supported structure has a fundamental frequency of $f = 1/2\pi * \sqrt{k/m}$. The corresponding angular frequency is thus $\omega = \sqrt{k/m}$. In the current work, both *ABP* and *WBP* are modeled. Thus the plate may have two wetted surfaces Ω_I (incident side) and Ω_B (back side). Consider normal incidence of an exponentially decaying planar pressure wave on the incident surface Ω_I:

$$p^i(x,t) = p_0 e^{-(t-x/c)/\theta} \tag{1}$$

where c is the speed of sound in water, p_0 is the peak pressure, and θ is the pressure decay time. Notice that origin of the coordinate is taken to be on the plate, with the positive direction to be the same as the traveling direction of the incoming wave. Based on the methodology presented in Liu & Young (2008), the equation of motion for the plate subject to planar shock wave reduces to the form typical of a mass-spring-damper system as follows:

$$m\ddot{u}(t) + \beta\rho c\dot{u}(t) + m\omega^2 u(t) - 2p_0 e^{-t/\theta} = 0 \tag{2}$$

where ρ is the water density. The velocity term in Eqn. 2 comes from the mass and momentum balance. Notice that in Eqn. 2, $\beta = 1$ for *ABP* and $\beta = 2$ for *WBP*. This difference is derived from the fact that the transmitted wave (given in Eqn. 5 of (Liu & Young, 2008) and Eqn. 9 of the current paper) is only relevant for *WBP*. The forcing term $2p_0 e^{-t/\theta}$ represents the summation of the incident and reflected pulses given that the plate is rigid and fixed in space. It should be pointed out that in Eqn. 2, the structural damping and fluid added-mass effects were neglected. In general, the effect of structural damping is negligible compared to acoustic damping. The effect of added-mass warrants further investigation. For early time response, the fluid acts as a compressible acoustic medium and localized added-mass effect should be considered; for late time response, the fluid acts more like an incompressible medium and global added-mass effect should be considered. One can expect that the added-mass effect is more important for late time response than for early time response. The current paper is mainly focusing on the early time response.

Applying initial conditions $u(0) = \dot{u}(0) = 0$ to solve for the transient structural response considering *FSI* from Eqn. 2:

$$\begin{aligned} u(t) = {} & \frac{p_0\theta^2}{m(1-M+K^2)}\{2e^{-t/\theta} \\ & + [-1 + \frac{2-M}{\sqrt{M^2-4K^2}}]e^{\frac{-M+\sqrt{M^2-4K^2}}{2}t/\theta} \\ & + [-1 - \frac{2-M}{\sqrt{M^2-4K^2}}]e^{\frac{-M-\sqrt{M^2-4K^2}}{2}t/\theta}\} \end{aligned} \tag{3}$$

$$\begin{aligned} \dot{u}(t) = {} & \frac{p_0\theta}{m(1-M+K^2)}\{-2e^{-t/\theta} \\ & + [-1 + \frac{2-M}{\sqrt{M^2-4K^2}}][\frac{-M+\sqrt{M^2-4K^2}}{2}]e^{\frac{-M+\sqrt{M^2-4K^2}}{2}t/\theta} \\ & + [-1 - \frac{2-M}{\sqrt{M^2-4K^2}}][\frac{-M-\sqrt{M^2-4K^2}}{2}]e^{\frac{-M-\sqrt{M^2-4K^2}}{2}t/\theta}\} \end{aligned} \tag{4}$$

$$\begin{aligned} \ddot{u}(t) = {} & \frac{p_0}{m(1-M+K^2)}\{2e^{-t/\theta} \\ & + [-1 + \frac{2-M}{\sqrt{M^2-4K^2}}][\frac{-M+\sqrt{M^2-4K^2}}{2}]^2 e^{\frac{-M+\sqrt{M^2-4K^2}}{2}t/\theta} \\ & + [-1 - \frac{2-M}{\sqrt{M^2-4K^2}}][\frac{-M-\sqrt{M^2-4K^2}}{2}]^2 e^{\frac{-M-\sqrt{M^2-4K^2}}{2}t/\theta}\} \end{aligned} \tag{5}$$

where the two non-dimensional parameters are defined as follows:

$$M \equiv \frac{\tau_S}{\tau_A} \equiv \frac{\theta}{\frac{m}{\beta\rho c}} = \frac{\beta\rho c\theta}{m} \tag{6}$$

$$K \equiv \frac{\tau_S}{\tau_V} \equiv \frac{\theta}{\frac{1}{\omega}} = \omega\theta \tag{7}$$

Notice that both M and K can be interpreted as the ratio between critical time scales. Basically, M is the ratio between the characteristic shock decaying time ($\tau_S = \theta$) and the characteristic

time to compress an acoustic medium with the same equivalent mass of the rigid plate ($\tau_A = m/\beta\rho c$); K is the ratio between the characteristic shock decaying time ($\tau_S = \theta$) and the characteristic free vibration time of the elastically supported plate ($\tau_V = 1/\omega$). Thus the inertial and elastic effects of the structural system subject to underwater shock loading are characterized by M and K, respectively.

After solving the structural response, the transient pressure on the incident surface Ω_I and on the back surface Ω_B can be obtained as, respectively:

$$p_I(t) = 2p_0 e^{-t/\theta} - \rho c\dot{u}(t) \tag{8}$$

$$p_B(t) = \rho c\dot{u}(t) \tag{9}$$

where $p_I(t)$ and $p_B(t)$ are respectively the pressure on the incident and back surfaces. Notice that $p_B(t)$ is only relevant for WBP.

It can be seen from Eqn. 2 that the system acts as a mass-spring-damper system. The value of the damping ratio determines the behavior of the system. It can be shown that:

1. $M/2K > 1$, the system is overdamped
2. $M/2K = 1$, the system is critically damped
3. $M/2K < 1$, the system is underdamped

The damping characteristics will be investigated in Section 3.2.

3 Results

As defined in Section 2, the two parameters M and K characterize the inertial and elastic effects, respectively. In this section, parametric studies will be performed to quantitatively study these two effects. In the following studies, the water density, sound speed, and steel density are chosen to be $\rho = 1000\ kg/m^3$, $c = 1400\ m/s$, and $\rho_s = 8000\ kg/m^3$, respectively. The incoming shock wave has peak pressure of $p_0 = 10\ MPa$ and pressure decay time of $\theta = 0.1\ ms$. Since a complete study was already presented in (Liu & Young, 2008) regarding the influence of back conditions, the current work will primarily focus on the water-backed structures.

3.1 Inertial effects

To study the inertial effects, the elastic effects are temporarily neglected, namely, $K = 0$ by taking $\omega = 0$. The plate is thus freely standing without elastic support. Three plate thicknesses are chosen to yield three distinct values for the inertial parameter M. These three values are respectively, $h_s = 0.001\ m$, $h_s = 0.01\ m$, and $h_s = 0.1\ m$, which lead to $m = 8\ kg/m^2$, $m = 80\ kg/m^2$, and $m = 800\ kg/m^2$, respectively. Correspondingly, the inertial parameter takes the value of $M = 35$, $M = 3.5$, and $M = 0.35$, respectively. Based on analytical results in (Liu & Young, 2008), cavitation is only relevant for WBP when $M < 2$. Thus among the above three cases, only the last one will lead to cavitation. The cavitation inception time can be calculated using the formula $\tau_c/\theta = [\ln M/(M-1) - \ln(2-M)/(M-1)]$ (Liu & Young, 2008). Even if cavitation is relevant for the thickest plate $h_s = 0.1\ m$, it will not occur until $t \approx 2.4\theta$. To avoid post-cavitation complications, the results in this section will only be plotted until $t = 2\theta$. Notice that in all the following plots, the time axis (horizontal) is normalized by the pressure decay time θ.

The inertial effects over the incident side shock pressure $p(t)$ is shown in Fig. 1. The pressure $p(t)$ is normalized by two times of the peak incident pressure p_0. In general, the pressure history is bounded by the case of infinity thickness ($h_s = \infty$ and thus $M = 0$) and the case of vanishing thickness ($h_s = 0$ and thus $M = \infty$). For the case of $M = 0$, the incident side shock pressure basically doubles the incoming pressure, namely, the plate is so thick (heavy) that it perfectly reflects the incoming pressure; for the case of $M = \infty$, the incident side shock pressure is equal to the incoming pressure, namely, the plate is so thin (light) that it appears transparent and completely passes the incoming pressure. The two cases ($M = 0.35$ and $M = 3.5$) are more intermediate. The case of $M = 35$ has a dog-leg shape in its pressure profile, namely a sharp drop in the initial stage followed by a gradual decay resembling the case of $M = \infty$, namely, the extremely thin (light) plate.

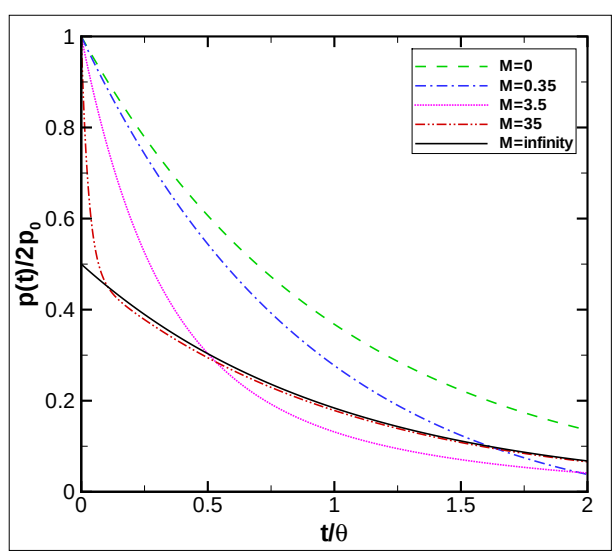

Figure 1. Inertial effects: the incident side shock pressure ($K = 0$).

The inertial effects over the plate momentum transfer is shown in Fig. 2. The unit area momentum $mv(t)$ is normalized by the maximum achievable momentum $2p_0\theta$ (Liu & Young, 2008). The normalized momentum transfer history is well bounded by the case of infinity thickness ($h_s = \infty$ and thus $M = 0$) and the case of vanishing thickness ($h_s = 0$ and thus $M = \infty$). For the case of $M = 0$, the momentum transfer is maximized, namely, it will reach the maximum momentum eventually (notice that only the first two decay time is shown so it is yet to reach the maxima of unity). This is because the plate is so thick (heavy) that it absorbs all the momentum that is available. For the case of $M = \infty$, the momentum transfer is zero, because the plate is so thin (light) that it allows the incoming pressure to escape without momentum loss. The two cases ($M = 0.35$ and $M = 3.5$) are more intermediate. The case of $M = 35$ ($h_s = 0.01m$) is already very close to the case of $M = \infty$ because of its thinness (lightness).

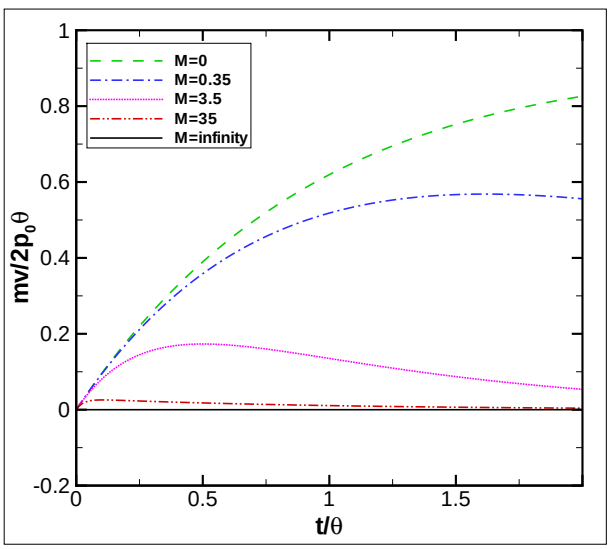

Figure 2. Inertial effects: the plate momentum transfer ($K = 0$).

3.2 Elastic effects

To study the elastic effects, the plate thickness is taken to be $h_s = 0.01\ m$, which leads to an inertial parameter of $M = 3.5$. Three characteristic frequencies are chosen to yield three distinct values for the elastic parameter K. These three frequency values are respectively, $f = 10^2\ Hz$, $f = 10^3\ Hz$, and $f = 10^4\ Hz$, which lead to $K = 0.02\pi$, $K = 0.2\pi$, and $K = 2\pi$, respectively. Since $M > 2$ so cavitation is not relevant, which permits the plotting of longer time without introducing complications. The following two figures are plotted until $t/\theta = 4$ to reveal all the essential features.

The inertial effects over the incident side shock pressure is shown in Fig. 3. In general, the pressure history is bounded by the case of infinity stiffness ($f = \infty$ and thus $K = \infty$) and the case of vanishing stiffness ($f = 0$ and thus $K = 0$). For the case of $K = \infty$, the incident side shock pressure basically doubles the incoming pressure, namely, the elastic support is so stiff (strong) that it prevents the plate from retreating and thus perfectly reflects the incoming pressure. The case of $K = 2\pi$ ($f = 10^4\ Hz$) features pressure oscillations. This is because $M/2K < 1$ and the system is underdamped. Its value is oscillating around that of the infinitely stiff plate $K = \infty$. Also noticed is that the magnitude of oscillation dies down quickly. After $t/\theta > 2$, it's essentially overlapping with the case of $K = \infty$ without much oscillation, primarily due to the acoustic damping effect. The case of $K = 0.02\pi$ ($f = 10^2\ Hz$) shows almost no difference than the case of $K = 0$ (the corresponding two curves are nearly indistinguishable). Thus the stiffness of the elastic support has to be high enough for the elastic effects to be significant. The case of $K = 0.2\pi$ ($f = 10^3\ Hz$) is more intermediate, showing noticeable difference than both the zero-stiffness and infinite-stiffness cases.

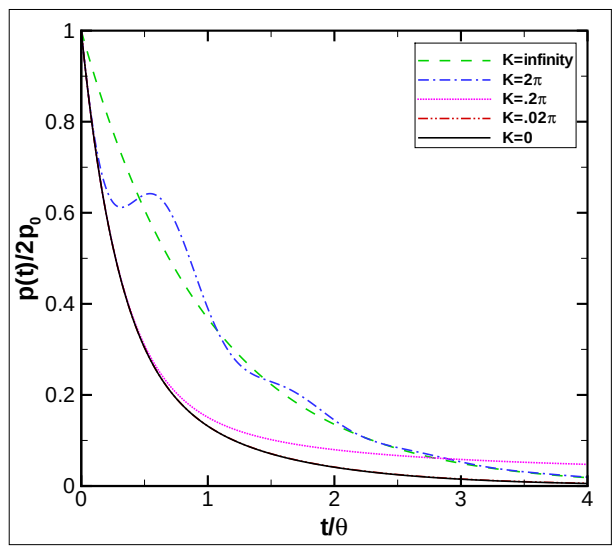

Figure 3. elastic effects: the incident side shock pressure ($M = 3.5$).

The inertial effects over the plate momentum transfer is shown in Fig. 4. In general, the momentum transfer history is also bounded by the case of infinity stiffness ($f = \infty$ and thus $K = \infty$) and the case of vanishing stiffness ($f = 0$ and thus $K = 0$). For the case of $K = \infty$, the plate momentum stays at zero. Physically, the elastic support is so stiff (strong) that it prohibits the plate with finite mass to move to gain momentum. In another word, the finite-thickness plate does not move at all while the

incoming pressure is doubled at the incident side. The case of $K = 2\pi$ features momentum transfer oscillations. This is again because $M/2K < 1$ and the system is underdamped. Its value is oscillating around that of the infinitely stiff plate $K = \infty$ (zero momentum transfer). Also noticed is that the magnitude of oscillation dies down quickly as well. After $t/\theta > 2$, it essentially becomes zero reflecting the fact of stationary plate, also due to the acoustic damping effect. The case of $K = 0.02\pi$ shows almost no difference than the case of $K = 0$ (the two legends are indistinguishable). The case of $K = 0.2\pi$ is more intermediate, with noticeably lower momentum transfer than the zero-stiffness plate.

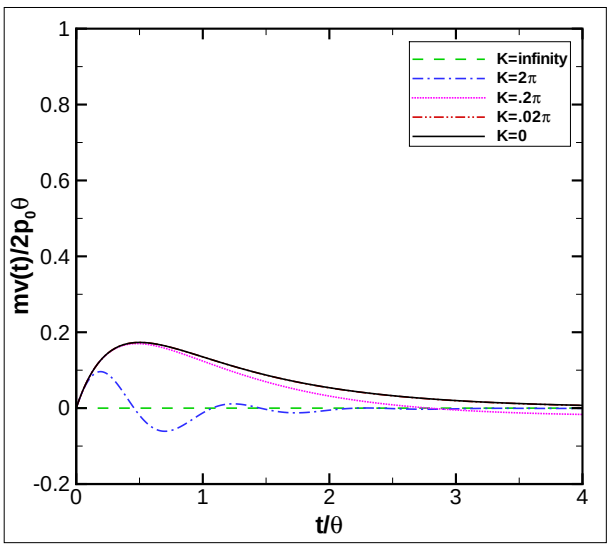

Figure 4. elastic effects: the plate momentum transfer ($M = 3.5$).

4 Discussions

Transient shock response of submerged plates with elastic support was analyzed. Inertial and elastic effects were investigated, which are characterized by two non-dimensional parameters, namely, the inertial parameter and the elastic parameter. Results show that:

1. The incident side shock pressure **increases** with the plate thickness (or mass per unit area) while all other conditions are fixed;
2. The plate momentum transfer **increases** with the plate thickness (or mass per unit area) while other conditions are fixed;
3. The incident side shock pressure **increases** with the stiffness of the elastic plate support while all other conditions are fixed;
4. The plate momentum transfer **decreases** with the stiffness of the elastic plate support while all other conditions are fixed.

ACKNOWLEDGEMENT

The authors are grateful to the Office of Naval Research (*ONR*) and Dr. Ki-Han Kim (program manager) for their financial support through grant numbers N00014-09-1-1204 and N00014-10-1-0296.

REFERENCES

HUTCHINSON, J. W. & XUE, Z. 2005 Metal sandwich plates optimized for pressure impulses. *Int. J. Mech. Sci.* **47**, 545–569.

KAMBOUCHEV, N., NOELS, L. & RADOVITZKY, R. 2006 Nonlinear compressibility effects in fluid-structure interaction and their implications on the air-blast loading of structures. *J. Appl. Phys.* **100**, 063519.

LIU, Z. 2008 Transient analysis and design of composite structures in multiphase flows. PhD thesis, Princeton University.

LIU, Z. & YOUNG, Y. L. 2008 Transient response of submerged plates subject to underwater shock loading : An analytical perspective. *J. Appl. Mech.* **75**, 044504.1–5.

LIU, Z. & YOUNG, Y. L. 2009 Utilization of bend-twist coupling for performance enhancement of composite marine propellers. *Journal of Fluids and Structures* **25**.

LIU, Z. & YOUNG, Y. L. 2010 Shock-structure interaction considering pressure precursor. In *28th Symposium on Naval Hydrodynamics*. California Institute of Technology.

TAYLOR, G. I. 1941 The pressure and impulse of submarine explosion waves on plates. *Scientific Papers of G I Taylor* **III**, 287–303.

YOUNG, Y. L. 2007 Time-dependent hydroelastic analysis of cavitating propeller. *Journal of Fluids and Structures* **23**.

YOUNG, Y. L. 2008 Fluid-structure interaction analysis of flexible composite marine propellers. *Journal of Fluids and Structures* **24**.